Supplementary Materials to:

Solvent mixing to induce molecular motor aggregation into bowl-shaped particles: underlying mechanism, particle nature and application to control motor behavior

Linda E. Franken[○‡], Yuchen Wei[◊^‡], Jiawen Chen[◊], Egbert J. Boekema[○], Depeng Zhao[◊], Marc C. A. Stuart[◊○]* and Ben L. Feringa[◊^]*

*Corresponding Authors

‡These authors contributed equally.

○ Electron Microscopy Group, Groningen Biomolecular Sciences and Biotechnology Institute, University of Groningen, Nijenborgh 7, 9747 AG Groningen, The Netherlands

◊ Centre for Systems Chemistry, Stratingh Institute for Chemistry, University of Groningen, Nijenborgh 4, 9747 AG Groningen, The Netherlands

^ Zernike Institute for Advanced Materials, University of Groningen, Nijenborgh 4, 9747 AG Groningen, The Netherlands

1. Materials and Methods

1.1 Spectroscopy

UV-vis spectra were recorded on a Hewlet-Packard HP 8543 Diode Array Photospectrometer or a Jasco V-630 spectrophotometer in a 1 cm pathlength quartz cuvette. Optical rotations were measured in CH_2Cl_2 with a 10 cm cell (c given in g/100 mL) and Schmidt+Haensch polarimeter (Polartronic MH8). CD spectra were recorded using a Jasco J-815 CD spectrophotometer. Fluorescence measurements were performed on a Jasco FP-6200 spectrophotometer. The UV irradiation experiments were conducted using a Spectroline model ENB-280C/FE lamp (8-watt) at 312 nm.

1.2 Dynamic light scattering

DLS was performed using a Dynapro nanostar, the results were analyzed with dynamics software, version 7 taking into account the viscosity of the THF-H_2O mixtures.[1]

1.3 Nile Red Fluorescence

Nile Red fluorescence was measured on an SPF-500c spectrofluorimeter (SLM Aminco) or a PTI International type C60/C-60 SE fluorimeter using an excitation wavelength of 490 nm. Fluorescent emission was measured from 510 to 700 nm at 5 or 1 nm intervals. The Nile Red emission maximum (λ max) was calculated using a log-normal fit.[2]

1.4 Characterization of THF in aggregates

The aggregates were prepared by adding 27 mL D_2O to the solution of 5 mg *trans*-stable **1** in 3 mL THF. The resulting mixture was then centrifuged (3000 rpm, 10 min) to separate the solids from the aqueous phase. To the isolated aggregates, D_2O (3 X 30 mL) was added, and the mixture was further sonicated and centrifuged until no THF was detected in D_2O by ^1H NMR. The washed aggregates were mounted into a NMR tube and dissolved with *d*-chloroform. NMR spectra were recorded using a Varian Mercury Plus, operating at 399.93 MHz for ^1H-NMR.

1.5 TEM and cryo-TEM

TEM and cryo-TEM images were made using two electron microscopes depending on availability. A Philips CM120 electron microscope (FEI, Eindhoven, the Netherlands) operated at 120 keV or a Tecnai G2 T20 electron microscope (FEI, Eindhoven, the Netherlands) operated at 200 keV. Both microscopes are equipped with an LaB6 cathode and 4K slow-scan CCD camera (Gatan, Pleasanton, CA, USA). Images were recorded using low-dose conditions. Three microliters of the sample solution was pipetted on glow-discharged copper grid coated with a continuous carbon film for negative staining with 2% uranyl acetate or drying (stability experiments). For cryo-TEM, the sample was applied to holey carbon film (quantifoil 3.5/1) and plunge-frozen with a Vitrobot (FEI, Eindhoven, The Netherlands) in liquid ethane after blotting for 5 s. The specimen was then inserted into a cryo-transfer holder (Gatan model 626). Each micrograph was cropped and had adjustments of levels, brightness, and contrast in Adobe Photoshop CS6.

1.6 Synthesis of Bulky First Generation Molecular Motor.

1.6.1 General remarks

Reagents were purchased from Aldrich, Acros, Merck or Fluka. Solvents were reagent grade and were distilled or dried before use according to standard procedures. Reactions were conducted under nitrogen atmosphere. Analytical TLC was performed with Merck silica gel 60 F254 plates and the visualization was done with UV light. Column chromatography was performed on silica gel (Merck silica gel 60, 230-400 mesh). NMR spectra were recorded using a Varian Mercury Plus, operating at 399.93 MHz for ^1H-NMR and 100.57 for ^{13}C-NMR. Chemical shifts were denoted in δ-units (ppm) relative to $HCCl_3$ (^1H-NMR: δ = 7.26 ppm; ^{13}C –NMR: δ = 77.16 ppm). For ^1H-NMR spectroscopy, the multiplicity is designated as follows: s (singlet), d (doublet), t (triplet), q (quatet), hept (heptet) m (multiplet), dd (doublet of doublets). HRMS spectra were obtained on a LTQ Orbitrap XL mass spectrometer with ESI ionization.

1.6.2 Synthesis

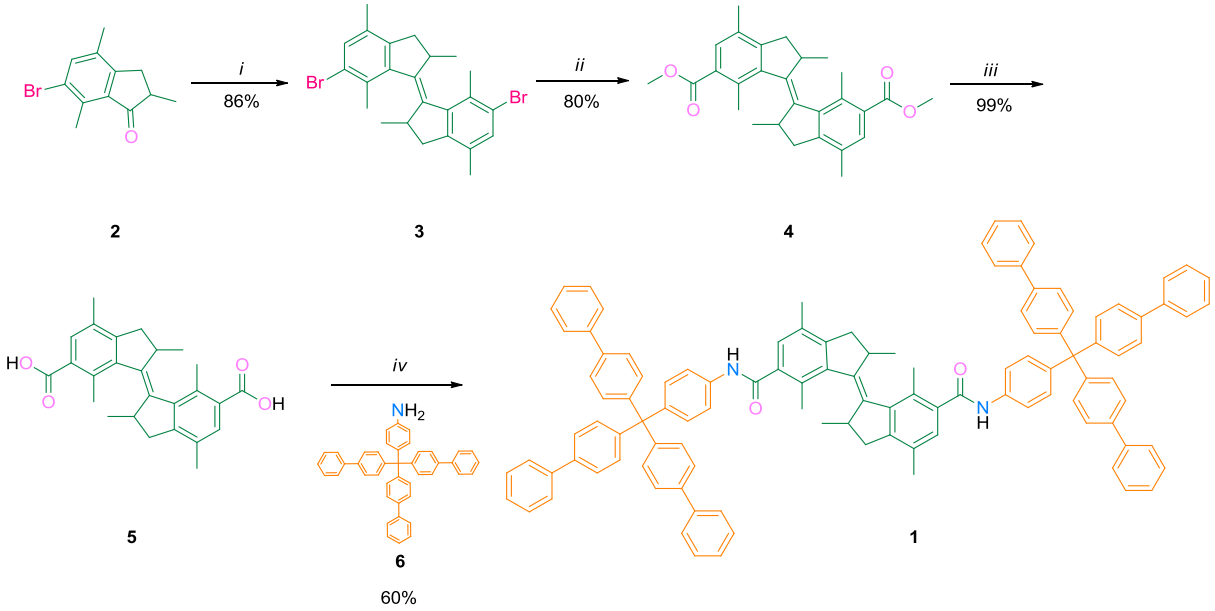

Scheme 1. Synthesis of bulky molecular motor 1. *i*) Zink powder, $TiCl_4$, reflux, 3d; *ii*) $Pd(dppp)_2Cl_2$, K_2CO_3, MeOH, NMP, CO(7.5 bar), 110 °C, 2d; *iii*) 1M aq. NaOH, MeOH, THF, 65 °C, 18h; *iv*) ① oxalyl chloride, DCM, THF, DMF, 0 °C, 1h; ② DCM, triethylamine, r.t., 18h.

The synthesis started with McMurry coupling of cycloketone **2**, which can be prepared according to a reported procedure,[3,4] to form the central olefin bond, giving the dibromo motor as a mixture of *trans*- and *cis*- isomers in 3:1 ratio. Palladium-catalyzed carbonylation, as reported, was employed to introduce esters onto the both sides of the motor.[5] At this stage, the two isomers could be separated with a total yield of 80% (60% for *trans*-**4** and 20% for *cis*-**4**).The hydrolysis of **4** in the presence of base resulted in the dicarboxylic acid **5** with almost quantitative yield. Compound **5** was then treated with oxalyl chloride with a catalytic amount of DMF, and the corresponding carbonyl chloride was directly used in the next step without any purification. After addition of the aniline **6**, of which the synthesis was already reported,[4] the desired molecular motor **1** was isolated.

Compound 3. To a suspension of zinc powder (2.0 g, 31.3 mmol) in dry THF (60 mL), $TiCl_4$ (1.63 mL, 14.8 mmol) was added at 0 °C. The resulting mixture was stirred at 65 °C for 2 h. After cooling down to room temperature, compound **2** (2.0 g, 8.0 mmol) was added and the resulting mixture was heated at reflux for another 3 days. The cooled mixture was poured onto silica and washed with DCM to remove the solids. After evaporation of the solvents, the crude product was purified by column chromatography using pentane / DCM (3:1) to give a *trans/cis*-mixture of compound **3** (1.6 g, 3.5 mmol, 86 % yield, *trans:cis* = 3:1) as a white solid.

Trans-**3**: ^{1}H NMR (400 MHz, Chloroform-*d*) δ 7.27 (s, 2H), 2.98 – 2.75 (m, 2H), 2.57 (dd, *J* = 14.7, 5.7 Hz, 2H), 2.45 (s, 6H), 2.22 (d, *J* = 11.1 Hz, 4H), 2.16 (s, 6H), 1.09 (d, *J* = 6.6 Hz, 6H).

Cis-**3**: ^{1}H NMR (400 MHz, CDCl3) δ 7.25 (s, 2H), 3.39 –3.29 (m, 2H), 3.04 (dd, *J* = 15.3, 6.4 Hz, 2H), 2.40 (d, *J* = 15.3 Hz, 2H), 2.23 (s, 6H), 1.51 (s, 6H), 1.08 (d, *J* = 6.1 Hz, 6H).

Compound 4. Dry methanol (2 mL) was added to the mixture of compound **3** (400 mg, 0.85 mmol, *trans:cis* = 3:1), potassium carbonate (258 mg, 1.87 mmol), Pd(dpppr)Cl_2 (50 mg, 0.08 mmol), and NMP (10 mL). The mixture was placed in autoclave under 7.5 bar CO, and heated at 110 ^{o}C for 2 days. After cooling to room temperature, the resulting mixture was diluted with water (10 mL) and then extracted with ether (2 X 20 mL). The combined organic layer was further washed with water (3 X 20 mL), brine (20 mL), and dried over Na_2SO_4. After evaporating the solvent *in vacuo*, and the residue was purified using column chromatography (pentane:ethyl acetate = 10:1) to give *trans*-stable **4** (222 mg, 0.52 mmol, 61 %) and *cis*-stable **4** (68 mg, 0.16 mmol, 19 %) as white solids.

Trans-stable **4**: ^{1}H NMR (400 MHz, Chloroform-*d*) δ 7.64 (s, 2H), 2.95 – 2.78 (m, 2H), 2.70 – 2.56 (m, 8H), 2.30 – 2.15 (m, 8H), 1.09 (d, *J* = 6.5 Hz, 6H).

Cis-stable **4**: ^{1}H NMR (400 MHz, Chloroform-*d*) δ 7.59 (s, 2H), 3.83 (d, *J* = 1.3 Hz, 6H), 3.44 – 3.35 (m, 2H), 3.12 (dd, *J* = 15.5, 6.5 Hz, 2H), 2.48 (d, *J* = 15.5 Hz, 2H), 2.28 (s, 6H), 1.65 (s, 6H), 1.08 (d, *J* = 6.7 Hz, 6H).

Compound 5. Compound *trans*-stable **4** (150 mg, 0.35 mmol) was dissolved in THF (2 mL), Methanol (2 mL), and aqueous NaOH (1M, 2 mL), followed by heating at 65 ^{o}C for 18 h. After cooling to room temperature, the mixture was titrated using HCl solution (1 M) to pH 3. Then the mixture was concentrated *in vacuo*, and the residue was dissolved in THF. The organic phase was collected of which the solvent was removed. The resulting white solid provided *trans*-stable **5** (142 mg, 0.35 mmol, 99%) without further purification. ^{1}H NMR (400 MHz, Methanol-d_4/DCM) δ 7.76 (s, 2H), 3.04 – 2.93 (m, 2H), 2.73 (s, 8H), 2.39 (d, *J* = 14.9 Hz, 2H), 2.31 (s, 6H), 1.19 (d, *J* = 6.5 Hz, 6H).

Cis-stable **5** (99 % yield) as a white solid was synthesized following the same procedures. ^{1}H NMR (400 MHz, Methanol-d_4) δ = 7.62 (s, 2H), 3.52 – 3.38 (m, 2H), 3.13 (dd, J = 15.4, 6.4 Hz, 2H), 2.56 (d, J = 15.4 Hz, 2H), 2.30 (s, 6H), 1.65 (s, 6H), 1.09 (d, J = 6.8 Hz, 6H).

Molecular motor 1. To a solution of *trans*-stable **5** (200 mg, 0.5 mmol) in THF (5 mL), DCM (5 mL), and DMF (1 drop) was add oxalyl chloride (0.21 mL, 2.5 mmol) at 0 ^{o}C under nitrogen. After warming up to room temperature, the mixture was stirred for another 1 h. The resulting solution was concentrated to yield acid chloride, which was subsequently dissolved in dry DCM (20 mL) and triethylamine (0.14 mL, 1 mmol). To the aforementioned solution of acid chloride, compound **6** (620 mg, 1.1 mmol) was added at 0 ^{o}C. After stirring at room temperature for 18 h, the resulting solution was washed with water (20 mL), brine (20 mL), and dried over Na_2SO_4. The solvents was evaporated *in vacuo*, and the resulting residue was purified by column chromatography (pentane:DCM = 1:1) to yield *trans*-stable **1** (449 mg, 0.3 mmol, 60 %) as a white solid. ^{1}H NMR (400 MHz, Chloroform-*d*) δ 7.66 – 7.50 (m, 30H), 7.48 – 7.30 (m, 34H), 7.20 (s, 2H), 2.98 – 2.90 (m, 2H), 2.66 (dd, *J* = 14.8, 5.7 Hz, 2H), 2.56 (s, 6H), 2.31 – 2.20 (m, 8H), 1.08 (d, *J* = 6.4 Hz, 6H). ^{13}C NMR (101 MHz, Chloroform-*d*) δ 168.76, 155.32, 145.72, 144.77, 142.70, 142.48, 141.84, 140.46, 138.60, 136.12, 135.79, 131.71, 131.58, 131.40, 129.40, 128.72, 127.21, 126.92, 126.20, 118.88, 63.93, 42.12, 39.00, 19.95, 18.79 , 18.15. HRMS (ESI+, m/z) calculated for $C_{112}H_{91}N_2O_2$ $[M + H]^+$ 1496.7109, found 1496.7127.

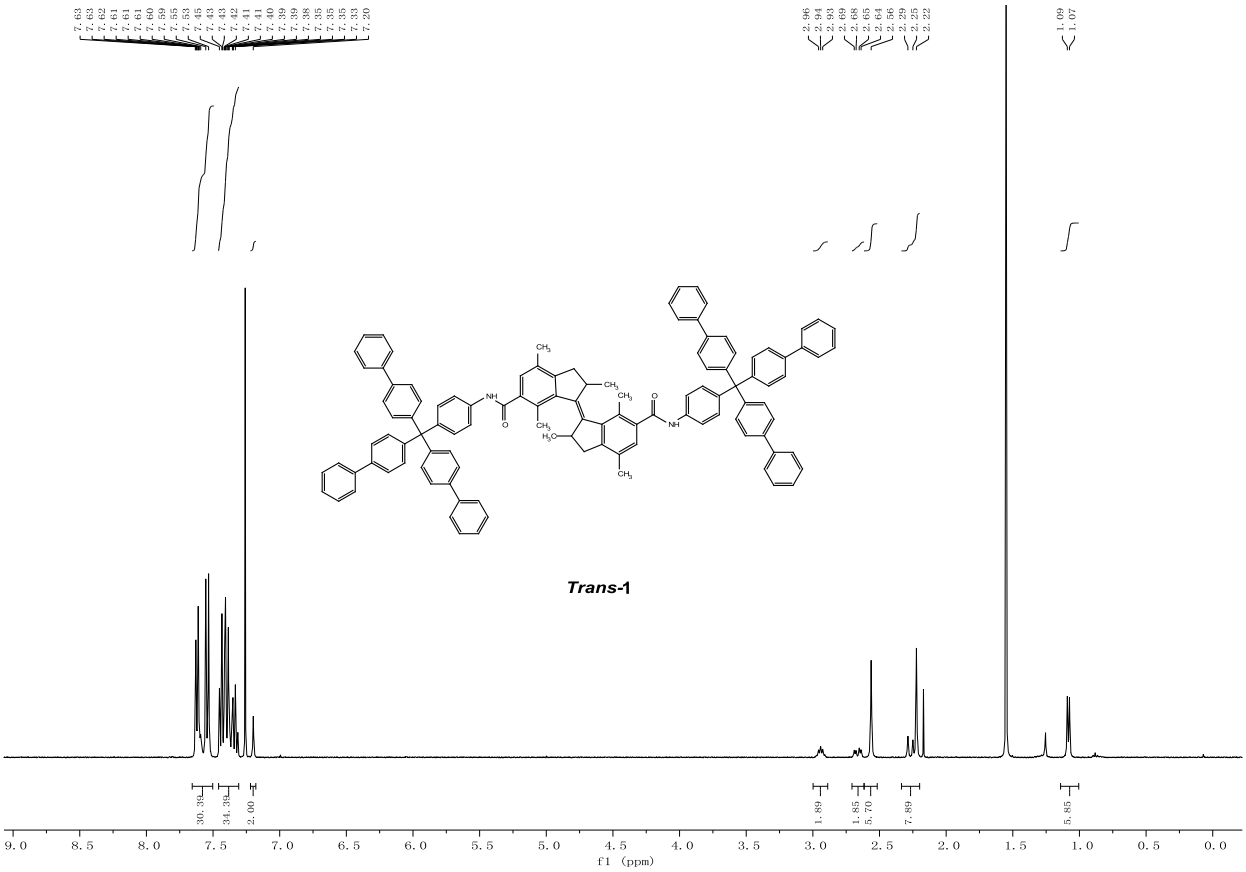

Figure S1. ^{1}H NMR spectrum of *trans*-stable **1** ($CDCl_3$).

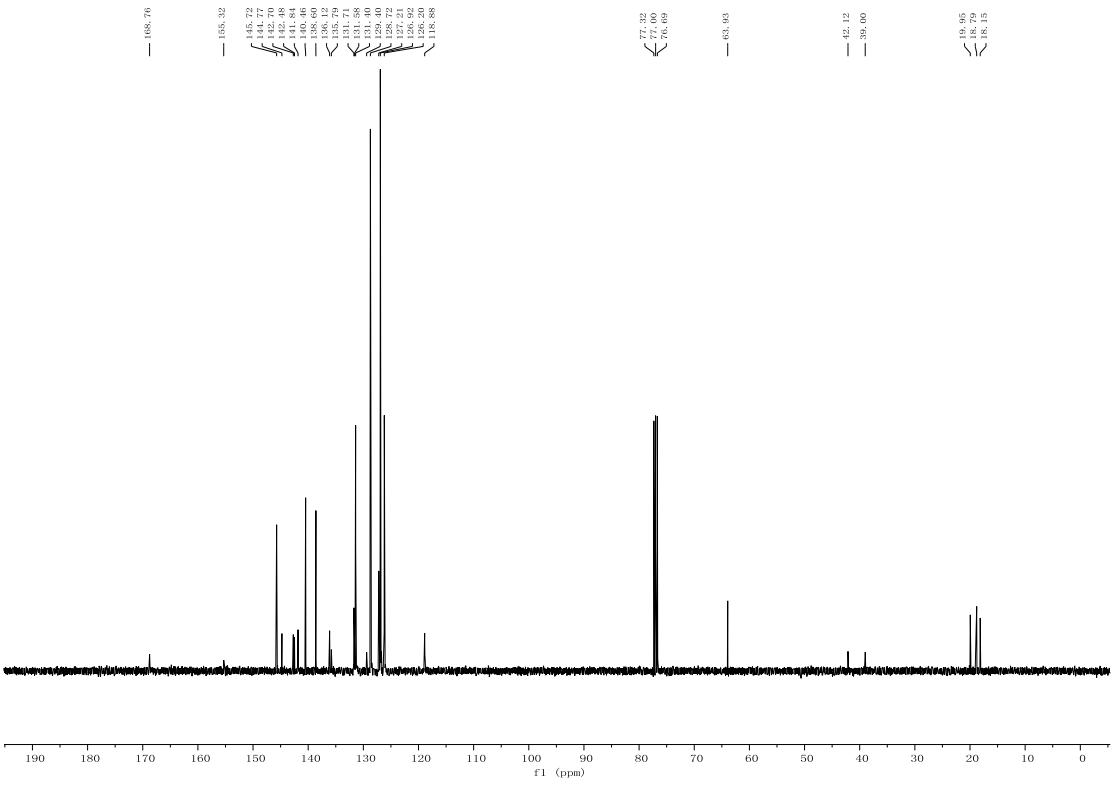

Figure S2. ^{13}C NMR spectrum of *trans*-stable **1** ($CDCl_3$).

Cis-stable **1** was obtained as a white solid with the same procedures and had a yield of 65 %. ^{1}H NMR (400 MHz, Chloroform-*d*) δ 7.86 – 7.80 (m, 2H), 7.69 – 7.60 (m, 4H), 7.56 – 7.49 (m, 12H), 7.48 – 7.27 (m, 46H), 7.23 (s, 2H), 3.50 – 3.34 (m, 2H), 3.16 (dd, *J* = 15.5, 6.2 Hz, 2H), 2.51 (d, *J* = 15.5 Hz, 2H), 2.29 (s, 6H), 1.12 (d, *J* = 6.6 Hz, 6H). ^{13}C NMR (101 MHz, Chloroform-*d*) δ168.60 , 146.21 , 145.81 , 142.55 , 142.29 , 141.18 , 140.52 , 138.46 , 136.10 , 131.43 , 131.30 , 130.18 , 128.74 , 128.66 , 127.41 , 127.12 , 126.95 , 126.16 , 126.04 , 119.43 , 63.93 , 41.01 , 39.06 , 20.12 , 19.12 , 18.22. HRMS (ESI+, m/z) calculated for $C_{112}H_{91}N_2O_2$ $[M + H]^+$ 1496.7109, found 1496.7127.

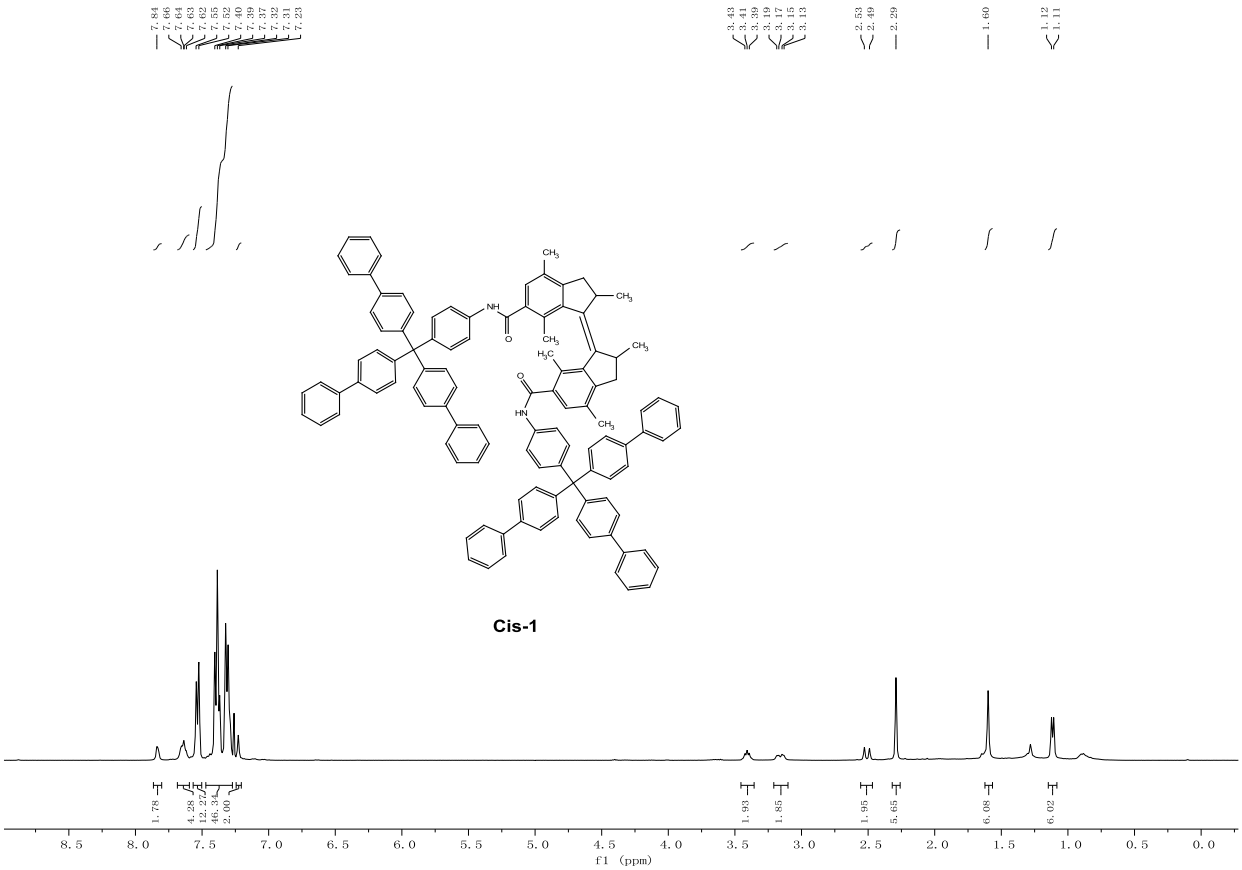

Figure S3. ^{1}H NMR spectrum of *cis*-stable **1** ($CDCl_3$).

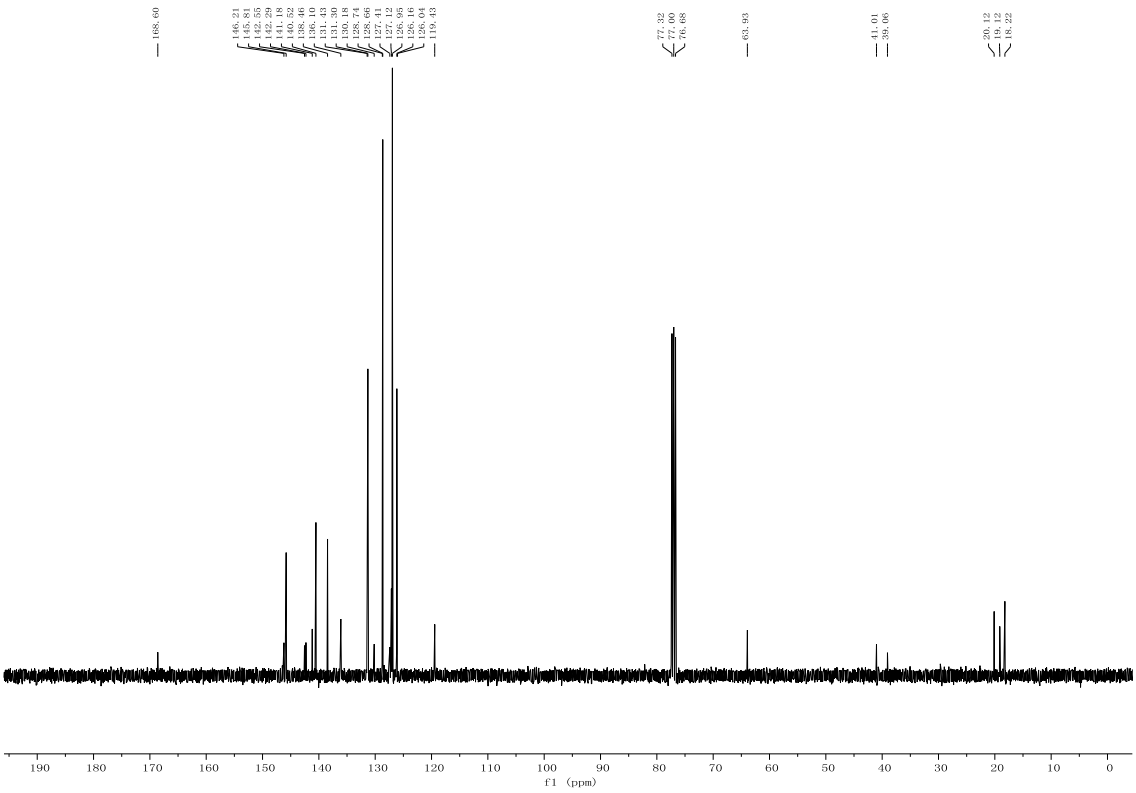

Figure S4. ^{13}C NMR spectrum of *cis*-stable **1** ($CDCl_3$).

(*R*,*R*)- (*P*,*P*)-*trans*-**5** and (*R*,*R*)- (*P*,*P*)-*cis*-**5** were prepared following a previous reported procedure.[3] Then, the same process was employed to synthesize (*R*,*R*)- (*P*,*P*)-*trans*-**1** and (*R*,*R*)- (*P*,*P*)-*cis*-**1** as that of the racemic material.

(*R*,*R*)- (*P*,*P*)-*trans*-**1:** 96% ee, $[\alpha]_D^{20}$ = -13.0 (c 0.2, CH_2Cl2).

(*R*,*R*)- (*P*,*P*)-*cis*-**1:** 96% ee, $[\alpha]_D^{20}$ = -15.2 (c 0.5, CH_2Cl2).

1.7 Freezing bath beads

As proof of principle of the proposed mechanism (figure 5) of bowl-shaped particle formation, we froze bath beads in liquid nitrogen to create similar bowl-shaped particles at a macroscopic-scale (Supplementary Movie 1). Upon freezing, the outer shell of the oil goes through the glass transition temperature and shrinks against the pressure from the still liquid interior resulting in a macroscopic bowl-shaped particle.

2. Supplementary figures

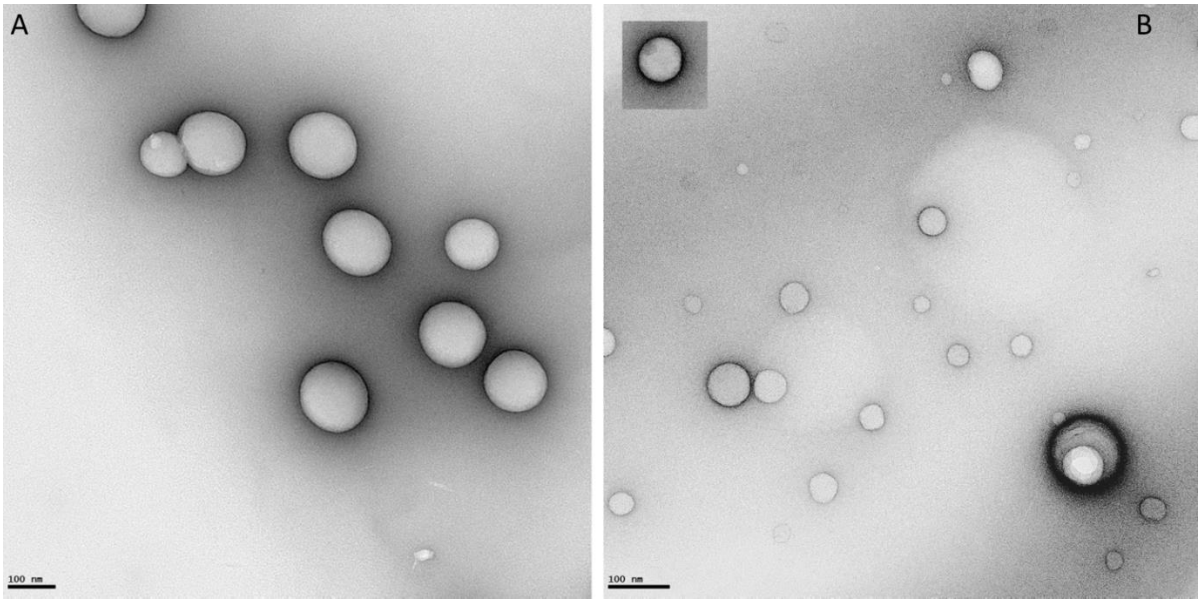

Figure S5. Solvent induced aggregation of 0.5 mg/ml Styrofoam in chloroform with 50% methanol (A) and of 0.6 mg/ml Nile Red in tertiary butanol with 75% water (B).

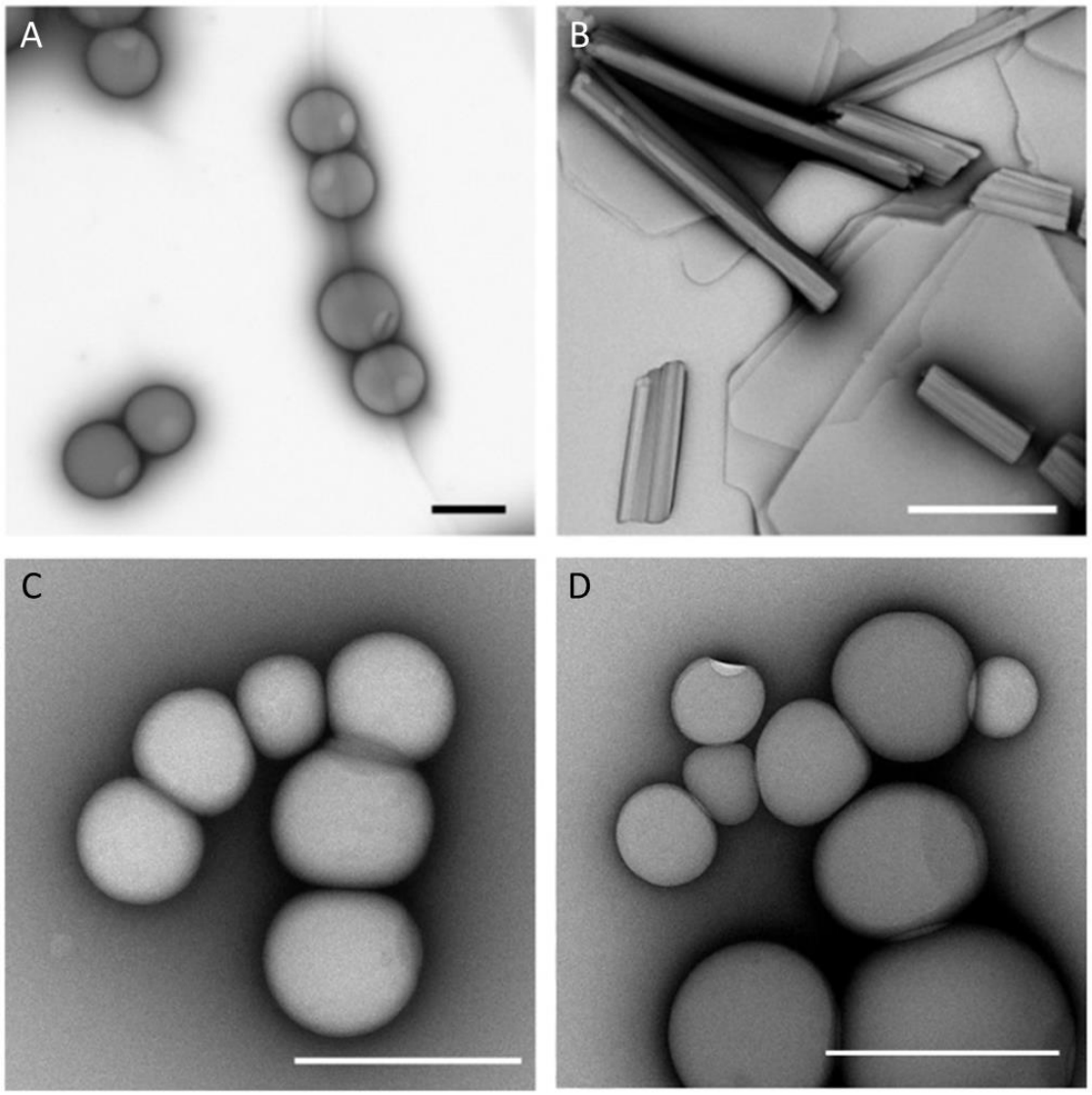

Figure S6. Spheres from the molecular motor 1 at 10^{-4} M in THF at ϕ_w 60% (A, B) and ϕ_w 90% (C, D), and their evolution over time. Panels B and D are images of samples A and C, respectively, after 4 days of aging. Scalebars represent 1 µm (black) and 500 nm (white), respectively.

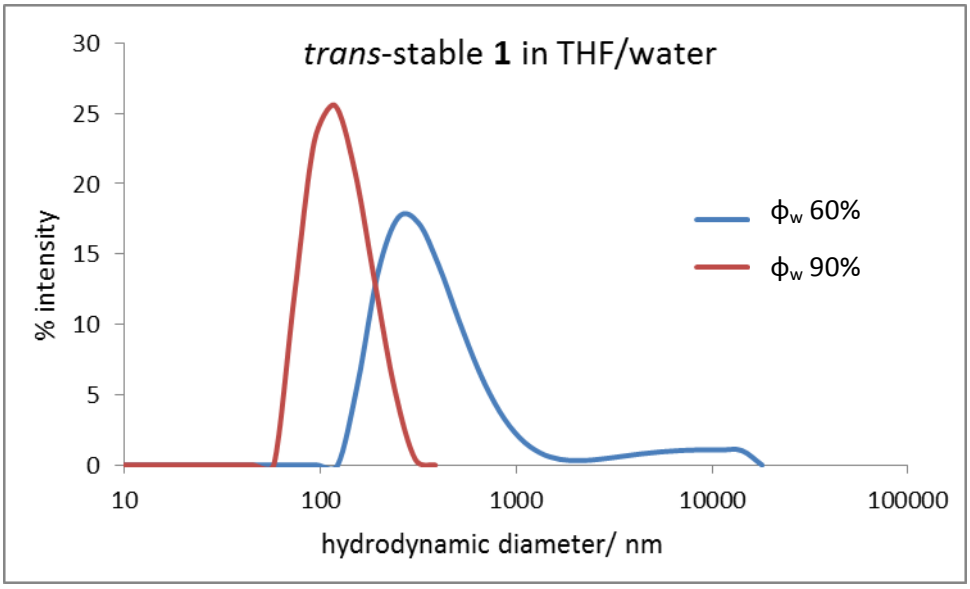

Figure S7. Particle size distribution of *trans*-stable **1** in THF/water mixture with ϕ_w = 60% and ϕ_w = 90% (c = 1 x 10^{-4} M). At 60% ϕw, a particle radius of 392 nm with a poly-dispersity of 64% is measured, whereas at 90% ϕw the radius is 130 nm with a polydispersity of 35%

2. Phase separation

In order to gain insight in the mechanism of bowl-shaped particle formation, we used Nile Red fluorescence to monitor the polarity dependent fluorescence maximum in different solvent-water mixtures[2](Figure S8). Measurements started at pure solvent (methanol, ethanol (not shown for figure clarity), propanol, tert-butanol and THF) and water was added stepwise. Only in methanol-water the absorption maximum keeps shifting linearly towards 660 nm (close to pure water[2]). In the other solvents at critical water content (CWC), the fluorescence spectrum suddenly broadened, showing a second population of Nile Red that experienced a much lower polarity. The hydrophobic Nile red does not tolerate the polarity of the water and initiates phase separation into droplets. As soon as the concentration of Nile Red is increased for TEM measurements, however, the CWC seems specific for the nature and concentration of the molecule and the nature of the initial solvent, rather than the water content. The fact that Nile Red does not cause precipitation into droplets in methanol underlines that not only the non-solvent, but also the solvent quality plays a role. While infinitely diluted Nile-Red results in droplets from the solvent being gathered around the hydrophobic Nile-Red, higher concentrations of Nile-Red in THF-water result in bowl-shaped particles at 75% ϕ_w (Figure 2B), indicating the role of hydrophobic interactions as well as a strong effect of molecular concentration.

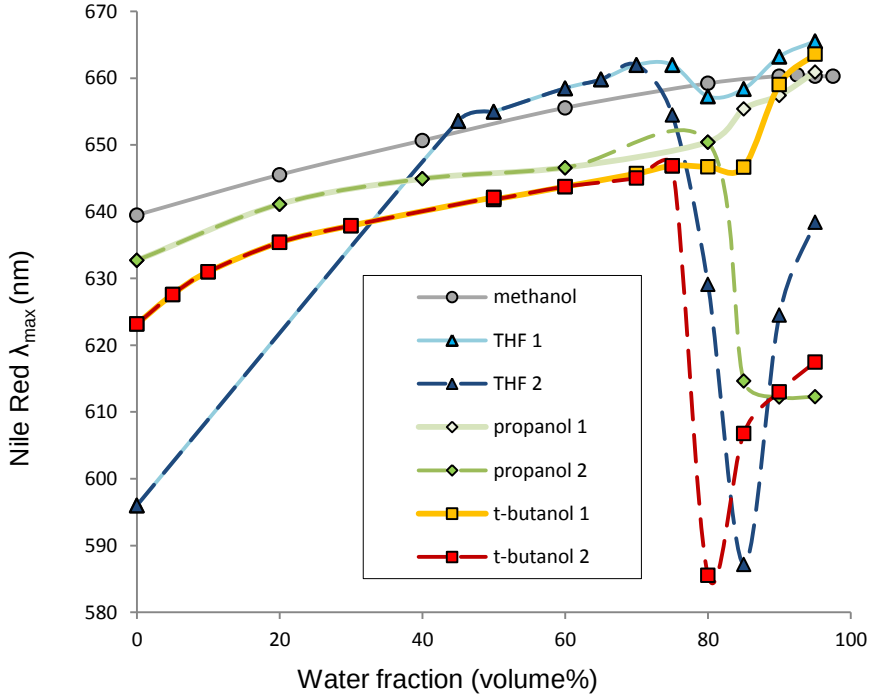

Figure S8. Nile Red fluorescence maxima, which change with polarity, of different solvent-water mixtures. Water acts as precipitator for Nile Red in all mixtures except methanol-water, inducing low-polarity droplets. At the CWC, the fluorescence spectra can not be explained with a single peak and are solved with convolution into two peaks (1 and 2), each peak representing a sub-population of the Nile Red.

A

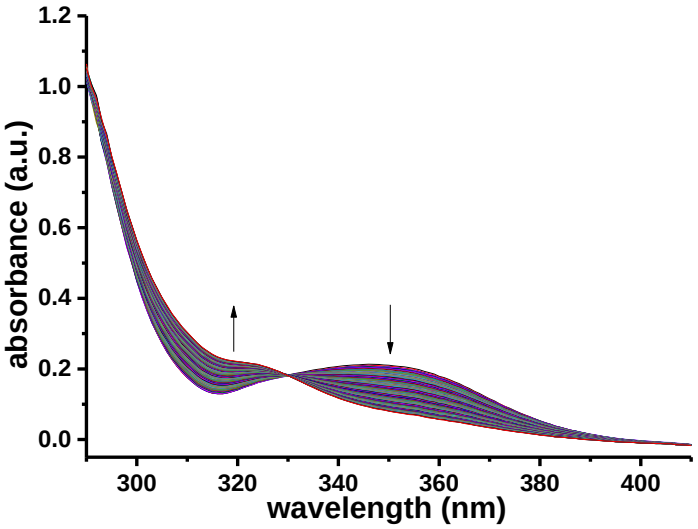

B

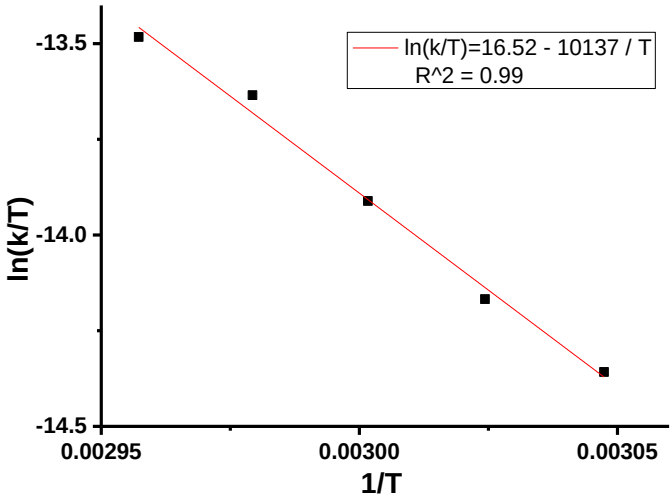

C

Δ‡Ho (kJ * mol -1)	**Δ‡So (J * mol-1 * K-1)**	**Δ‡Go (kJ * mol-1)**	**t1/2 (h)**
84.3±4.2	-60.2±5.5	102.2±4.2	26

Figure S9. Kinetic measurements of the thermal isomerization **step 2** in THF. (A) UV/vis spectral changes during heating at 55 °C. (B) The linear fitting of ln (k/T) by 1/T using Erying equation $\ln\frac{k}{T} = \frac{-\Delta H^{\ddagger}}{R}\cdot\frac{1}{T} + \ln\frac{k_B}{h} + \frac{\Delta S^{\ddagger}}{R}$. The rate constants of the first-order decay *k* were obtained from equation A/Ao = e^{-kt}, at 55 °C, 57.5 °C, 60 °C, 62.5 °C, and 65 °C. (C) The calculated standard enthalpy **Δ‡H°**, entropy **Δ‡S°**, Gibbs energy **Δ‡G°** of activation, and the half-life of cis-unstable **1** at 298.15 K.

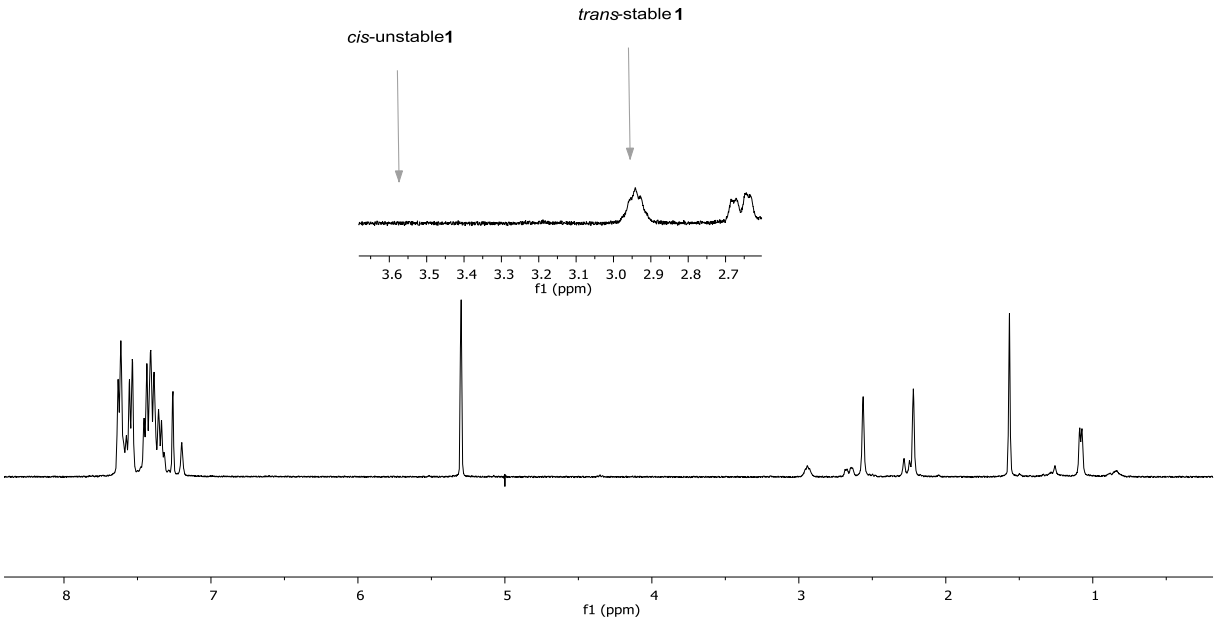

Figure S10. ^{1}H NMR spectrum of the powder of *trans*-stable **1** after 2h irradiation with 312 nm UV light. No *cis*-unstable **1** is observed.

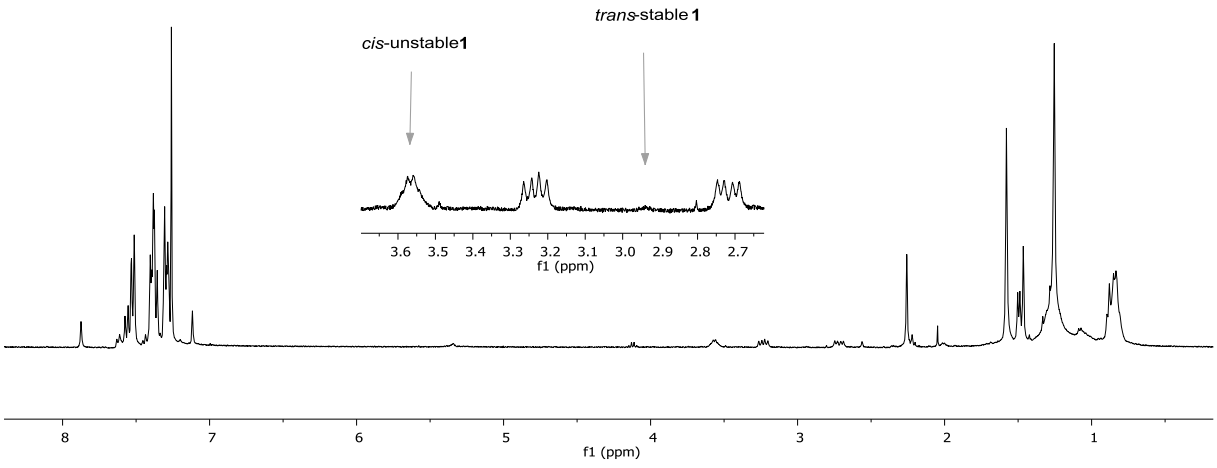

Figure S11. ^{1}H NMR spectrum of solid *cis*-unstable **1** after 48h. *Trans*-stable **1** in $CDCl_3$ was irradiated to its PSS with 312 nm UV light. After fast evaporating the solvent, the solid was placed at 50 ^{o}C for 48h which was then used for NMR. No significant *cis*-stable **1** is observed.

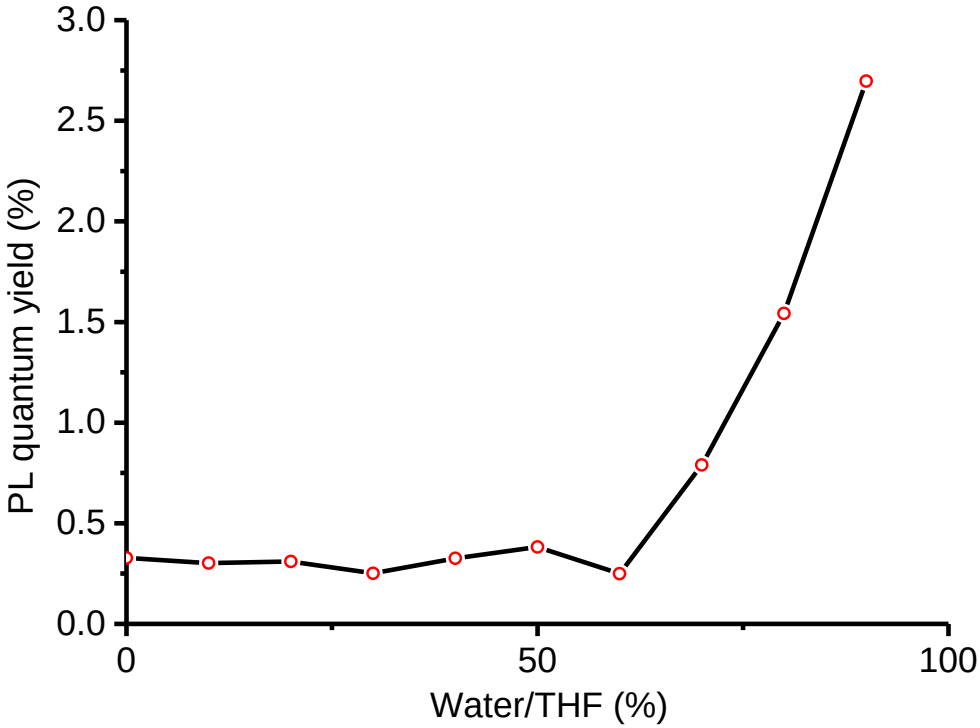

Figure S12. AIE quantum yields of *cis*-unstable **1** determined by comparison with a standard compound (quinine in 0.05 M H_2SO_4 solution).

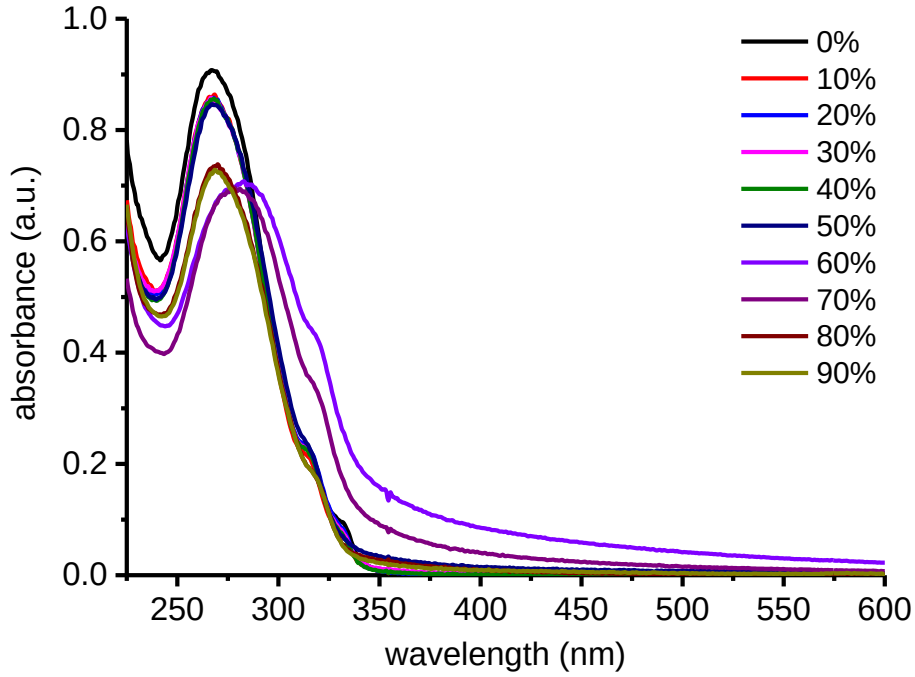

Figure S13. UV-vis absorption spectra of *trans*-stable **1** in THF/water mixture with different ϕ_w (c = 3 x 10^{-6} M).

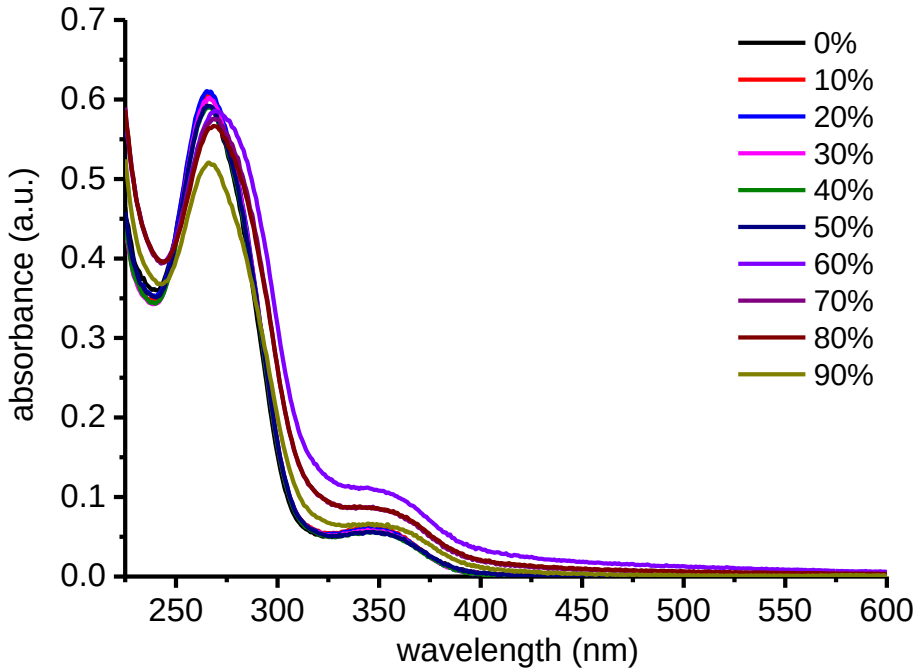

Figure S14. UV-vis absorption spectra of *cis*-unstable **1** in THF/water mixture with different ϕ_w (c = 3 x 10^{-6} M).

A

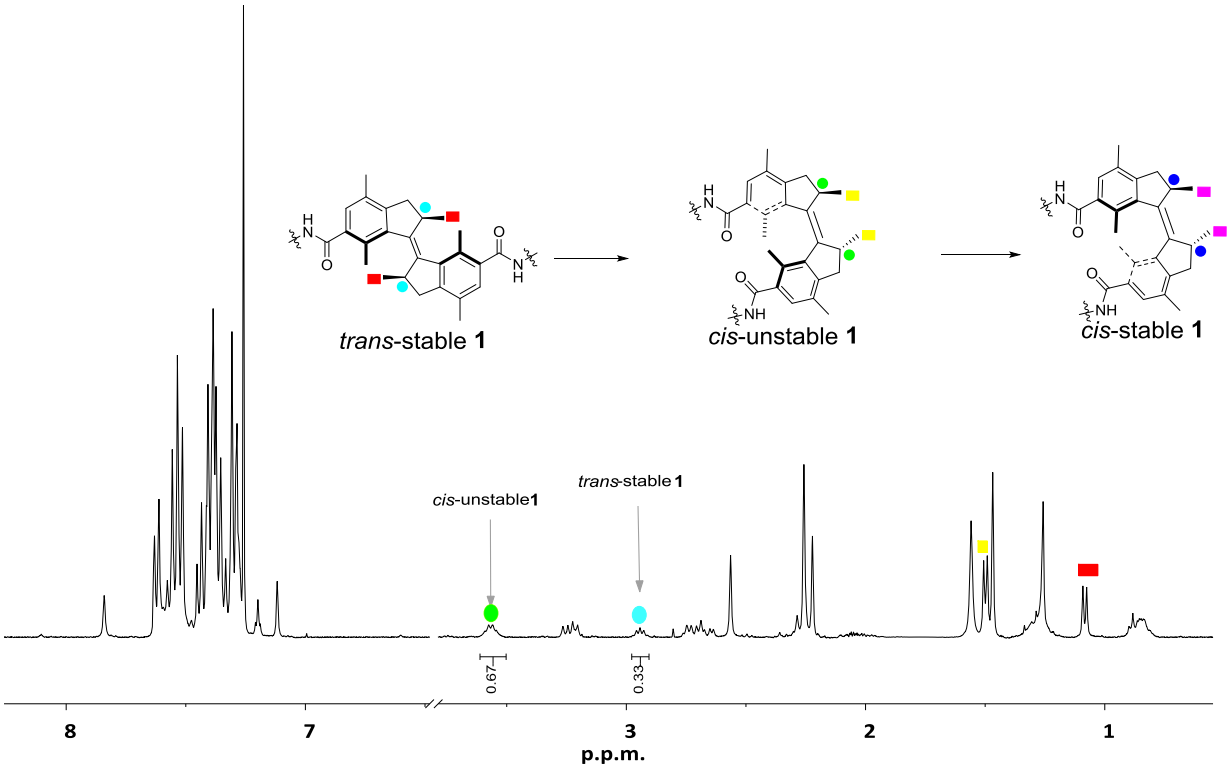

B

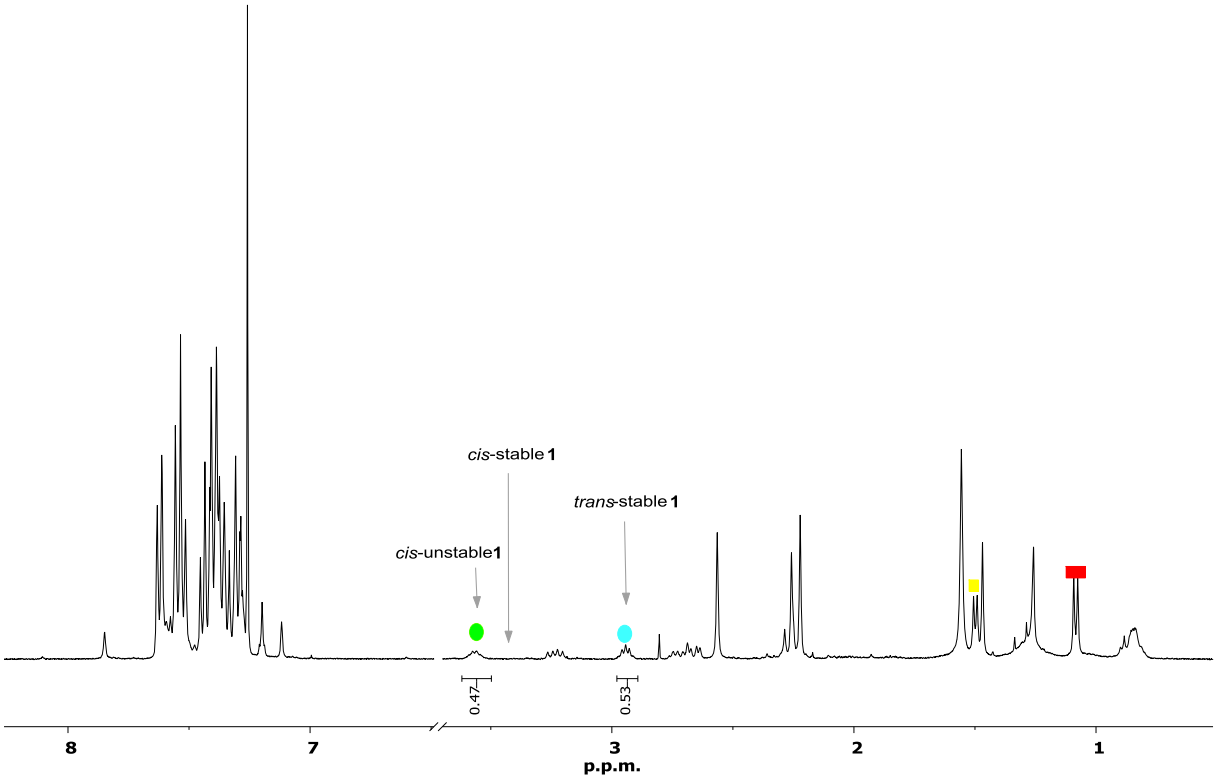

Figure S15. ^{1}H NMR spectra ($CDCl_3$) of (A) PSS after irradiating *trans*-stable **1** aggregates (ϕ_w = 90 %) with 312 nm UV light for 1 h and (B) the resulting THI at 50 ^{o}C for 48h.

A

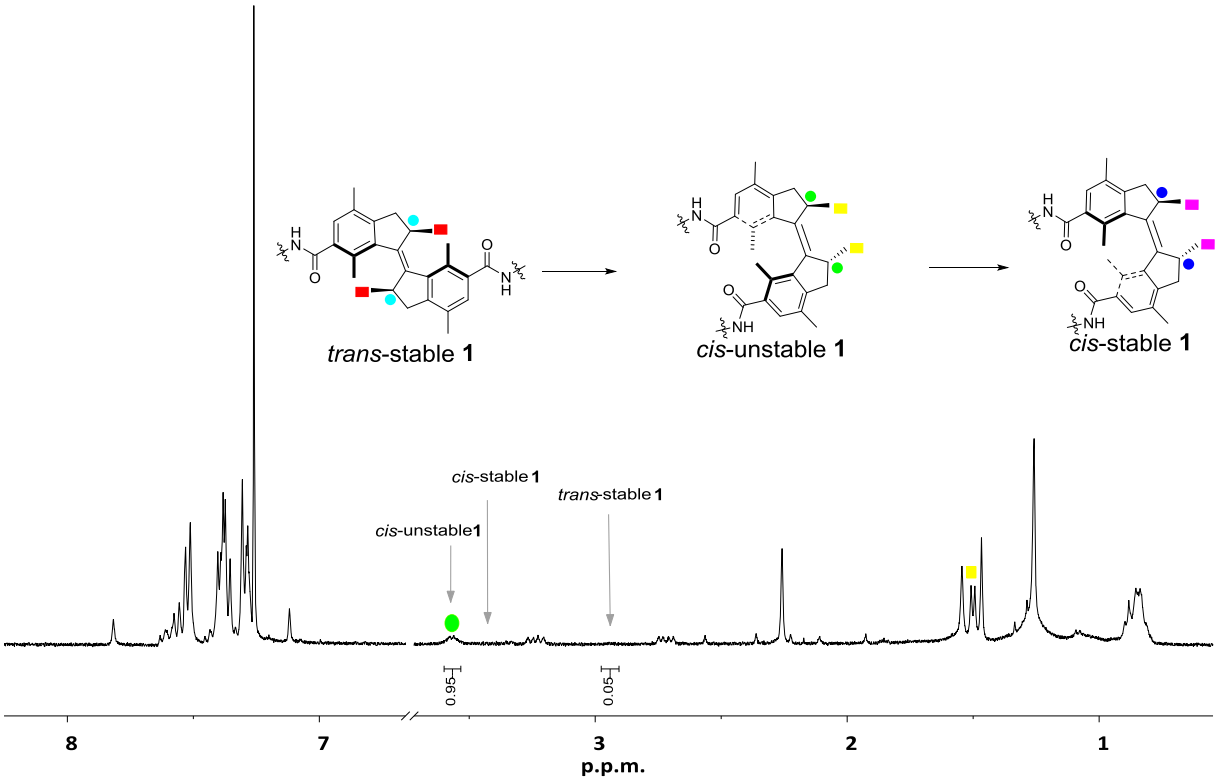

B

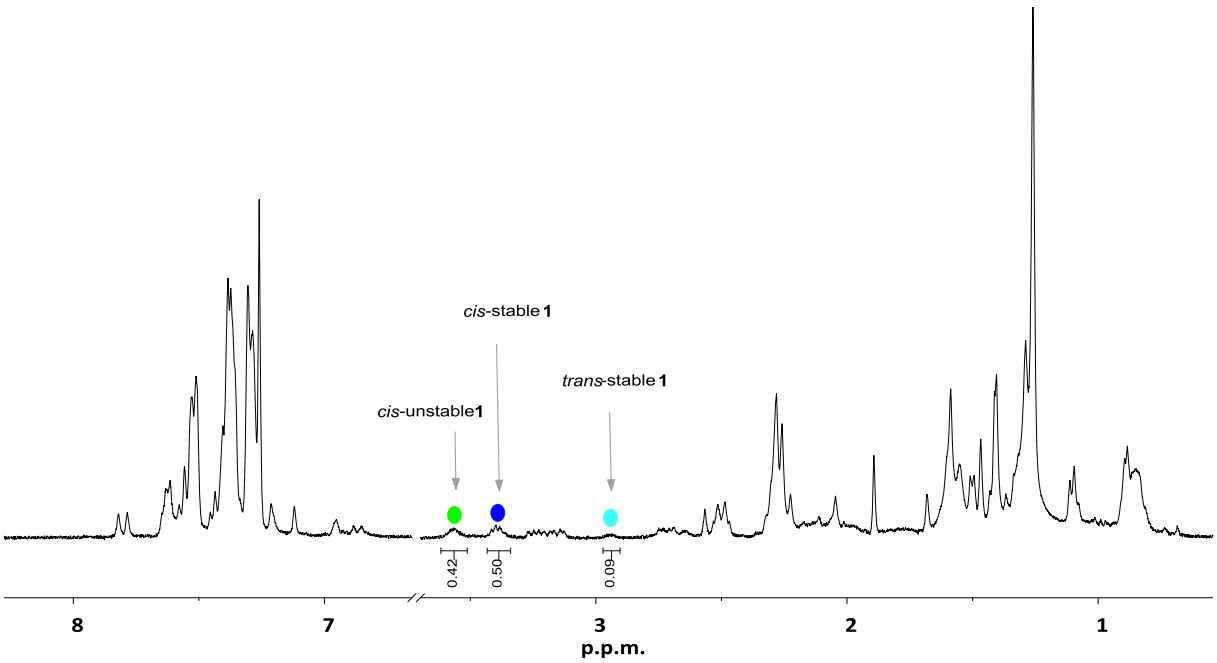

Figure S16. ^{1}H NMR spectra ($CDCl_3$) of (A) PSS after irradiating *trans*-stable **1** aggregates (ϕ_w = 60 %) with 312 nm UV light for 30 min and (B) the resulting THI at 50 ^{o}C for 24h.

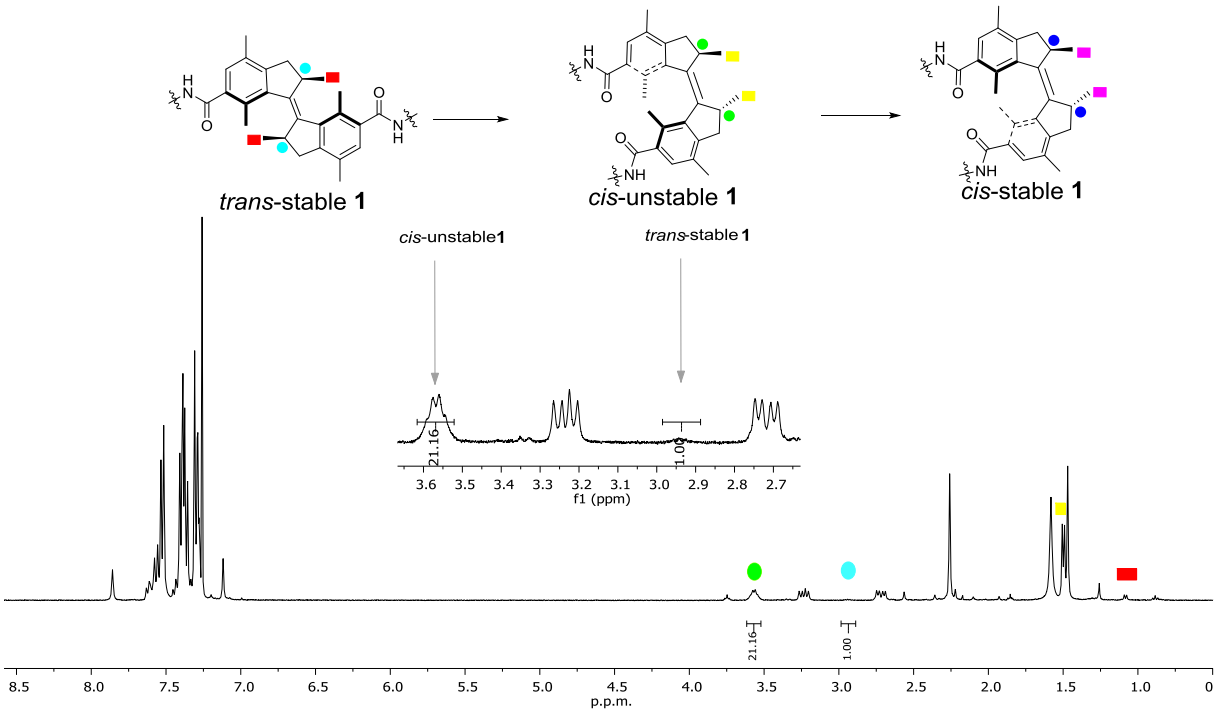

Figure S17. ^{1}H NMR spectrum of *cis*-unstable **1** in the aggregates (ϕ_w = 90%) after heating. *Trans*-stable **1** was irradiated to PSS in THF which was followed by adding water. The resulting mixture was heated at 50 ^{o}C for 48h. The aggregates were then centrifuged and dissolved in $CDCl_3$ for NMR.

3. References

(1) Hao, J.; Cheng, H.; Butler, P.; Zhang, L.; Han, C. C. Origin of cononsolvency, based on the structure of tetrahydrofuran-water mixture. *J. Chem. Phys.* **2010***, 132*, 154902.

(2) Stuart, M.; van de Pas, J.; Engberts, J. The use of Nile Red to monitor the aggregation behavior in ternary surfactant-water-organic solvent systems. *Journal of Physical Organic Chemistry* **2005***, 18*, 929-934.

(3) Kaminsky, W.; Rabe, O.; Schauwienold, A. M.; Schupfner, G. U.; Hanss, J.; Kopf, J. Crystal structure and propene polymerization characteristics of bridged zirconocene catalysts. *J. Organomet. Chem.* **1995**, *497* (1–2), 181.

(4) Wang, J.; Kulago, A.; Browne, W. R.; Feringa, B. L. Photoswitchable Intramolecular H-Stacking of Perylenebisimide. *J. Am. Chem. Soc.* **2010**, *132* (12), 4191.

(5) Zhao, D.; Neubauer, T. M.; Feringa, B. L. Dynamic control of chirality in phosphine ligands for enantioselective catalysis. *Nat. Commun.* **2015**, *6*, 6652.

(6) Bonardi, F.; Halza, E.; Walko, M.; Du Plessis, F.; Nouwen, N.; Feringa, B. L.; Driessen, A. J. M. Probing the SecYEG translocation pore size with preproteins conjugated with sizable rigid spherical molecules. *Proc. Natl. Acad. Sci. U. S. A.* **2011**, *108* (19), 7775.